MATHEMATICAL METHODS IN THE APPLIED SCIENCES
Math. Meth. Appl. Sci. 2004; **27**:1545–1565 (DOI: 10.1002/mma.514)
MOS subject classification: 35 K 65; 65 N 40; 53 C 80

A direct method for solving an anisotropic mean curvature flow of plane curves with an external force

Karol Mikula[1,*,†] and Daniel Ševčovič[2,‡]

[1]*Department of Mathematics, Slovak University of Technology, Radlinského 11, 813 68 Bratislava, Slovak Republic*
[2]*Institute of Applied Mathematics, Faculty of Mathematics, Physics & Informatics, Comenius University, 842 48 Bratislava, Slovak Republic*

Communicated by G. Dziuk

SUMMARY

A new method for solution of the evolution of plane curves satisfying the geometric equation $v=\beta(x,k,v)$, where v is the normal velocity, k and v are the curvature and tangential angle of a plane curve $\Gamma\subset\mathbb{R}^2$ at the point $x\in\Gamma$, is proposed. We derive a governing system of partial differential equations for the curvature, tangential angle, local length and position vector of an evolving family of plane curves and prove local in time existence of a classical solution. These equations include a non-trivial tangential velocity functional governing a uniform redistribution of grid points and thus preventing numerically computed solutions from forming various instabilities. We discretize the governing system of equations in order to find a numerical solution for 2D anisotropic interface motions and image segmentation problems. Copyright © 2004 John Wiley & Sons, Ltd.

KEY WORDS: mean curvature flow; anisotropy; external force; interface; image segmentation; Lagrangian approach; semi-implicit scheme

1. INTRODUCTION

In this paper, we study the evolution of a closed smooth embedded plane curve $\Gamma: S^1\to\mathbb{R}^2$. The normal velocity v of an evolving family of plane curves Γ_t, $t\geqslant 0$, is assumed to be a function of the curvature k, tangential angle v and position vector $x\in\Gamma_t$,

$$v=\beta(x,k,v) \tag{1}$$

*Correspondence to: Karol Mikula, Department of Mathematics, Slovak University of Technology, Radlinského 11, 813 68 Bratislava, Slovak Republic.
†E-mail: mikula@vox.svf.stuba.sk
‡E-mail: sevcovic@fmph.uniba.sk

Contract/grant number: VEGA No. 1/0313/03
Contract/grant number: VEGA 1/0259/03
Contract/grant number: SFB 359

Published online 17 May 2004

Received 12 March 2002

Geometric equations of the form (1) appear within a large variety of applied problems as dynamics of phase boundaries in thermomechanics, in modelling of flame front propagation, in combustion, semiconductors industry, etc. They also have a special importance in image processing and computer vision. A particular choice $v = \beta(k)$ leads to the so-called morphological image and shape multiscale analysis studied by Alvarez *et al.* [1]. Sapiro and Tannenbaum [2] considered a special choice of the normal velocity $\beta(k) = k^{1/3}$ for the affine invariant analysis of shapes. A typical case in which the normal velocity v may depend on the position vector x can be found in image segmentation [3,4]. For a comprehensive overview of other important applications of the geometric equation (1) we refer to recent books by Sethian [5], Sapiro [6] and Osher and Fedkiw [7].

We follow the so-called direct approach for solving the geometric equation (1). In comparison to the other well-known techniques, like, e.g. level-set method [5,7,8] or phase-field approximations (see e.g. References [9,10]), in the direct approach one-space-dimensional evolutionary problems are solved. A first idea behind the direct approach consists of representation of a family of embedded curves Γ_t by the position vector $x \in \mathbb{R}^2$, i.e. $\Gamma_t = \mathrm{Image}(x(.,t))$ where x is a solution to the geometric equation

$$\partial_t x = \beta \mathbf{N} + \alpha \mathbf{T} \tag{2}$$

where $\beta = \beta(x, k, v)$, $\mathbf{N} = (-\sin v, \cos v)$ and $\mathbf{T} = (\cos v, \sin v)$ are the unit inward normal and tangent vectors, respectively. For the normal velocity $v = \partial_t x.\mathbf{N}$ we have $v = \beta(x, k, v)$. Notice that the presence of a tangential velocity functional α has no impact on the shape of evolving curves and therefore a 'natural' setting $\alpha = 0$ has been chosen for analytical as well as numerical treatment in the literature [11–15]. An important role of a non-trivial tangential term has been discovered and utilized in References [16–21]. In Reference [21], Equation (1) has been solved with $\beta = \beta(k, v)$ non-linearly depending on the curvature k. The tangential term α appearing in (2) has been chosen in such a way that an initial distribution of grid points representing a curve is preserved during evolution. In case of isotropic and linear dependence of the flow on curvature, the same redistribution strategy has been suggested by Hou *et al.* in References [16,19]. Such an approach significantly improved and stabilized all computations realized by the direct method which has been documented by a variety of numerical experiments in References [16,19,21].

Here, we present a direct method for solving the geometric equation (1) with the normal velocity v involving a curvature, anisotropy, spatial position dependence and strong external driving force. In the case of a convex initial curve such an approach was discussed in References [22,23] where the so-called curve shortening equation has been solved in a fixed spatial interval determined by a range of values of the tangential angle. In the non-convex case the situation is more difficult because the tangential angle cannot be used as a fixed domain parametrization. However, as it will be shown in this paper for general situation (1), a closed system of equations for both geometrical quantities k and v can be derived enabling us to handle evolution of non-convex curves also. Particular cases of such equations have been considered in References [16,19] for linear curvature driven motions and in Reference [21] for anisotropic non-linear curvature flows without spatial dependence of the evolution. The system contains intrinsic parabolic equations for the curvature, tangential angle and ordinary differential equations for evolution of the local length element and position vector. The governing system includes a non-trivial tangential velocity functional α which in comparison to References [16,19,21] forces a curve representation to be uniform without any condition

to its initial grid points distribution. Taking into account such suitable tangential velocity we can prevent numerical solutions from forming numerical instabilities like, e.g. merging of grid points or formation of 'swallow tails'. We can furthermore resolve the so-called sharp corners formation and their evolution. From the analytical point of view, we prove short time existence of solution to a general non-linear curve evolution model (1) and derive further properties of solutions like, e.g. existence of various Lyapunov functionals.

Our suggested fully discrete numerical scheme is semi-implicit in time, i.e. all non-linearities are treated from the previous time step and linear terms are discretized at the current time level. Then we solve tridiagonal systems in every time step in a fast and simple way. We show that the stability constraint for our semi-implicit scheme with tangential redistribution is related to an integral average of $k\beta$ along the curve and not to pointwise values of $k\beta$. The pointwise influence of this term would lead to severe time step restriction in a neighbourhood of corners, while our approach benefits from a regularity of the curve outside the corners. Thus the method allows the choosing of larger time steps without loss of stability.

The outline of the paper is as follows. In the next section, we discuss applications in which a geometric equation of form (1) naturally occurs. In Section 3, we present a governing system of PDEs capable of describing the evolution of plane curves satisfying (1). We prove local in time existence of classical solutions by means of the abstract theory of fully non-linear parabolic equations. Section 4 is devoted to the study of qualitative properties of solutions. We derive several Lyapunov functionals decreasing along trajectories. Section 5 is focused on the problem of how to choose a suitable tangential velocity functional α. In Section 6, numerical schemes for full space time discretization of the governing system of equations are presented and the results of numerical simulations are discussed.

2. MOTIVATION

Throughout the paper we will be mainly concerned with applications in which the normal velocity v may depend on the position vector x, the tangential angle ν and the dependence on the curvature k is linear, i.e. $v=\beta(x,k,\nu)$ where

$$\beta(x,k,\nu)=\delta(x,\nu)k+c(x,\nu) \tag{3}$$

and $\delta>0$ and c are smooth coefficients depending on x and ν.

The sharp-interface description of the solidification process is described by the Stefan problem with a surface tension, i.e. the heat equation is solved in both phases, the Stefan condition for heat fluxes on the interface is taken into account and the Gibbs–Thomson law for interface motion in the form

$$\frac{\delta e}{\sigma}(U-U^*)=-\gamma_2(\nu)k+\gamma_1(\nu)v \tag{4}$$

where v is the normal velocity of the interface, k its curvature, U^* is a melting point, δe is difference in entropy per unit volume between liquid and solid phases, σ is a constant surface tension, γ_1 is a coefficient of attachment kinetics and dimensionless function γ_2 describes anisotropy of the interface is considered (see e.g. References [10,24]). One can see that the Gibbs–Thomson condition can be viewed as a relationship of the form (3). In Reference [13], Angenent and Gurtin studied perfect conductors where the problem can be reduced to a single

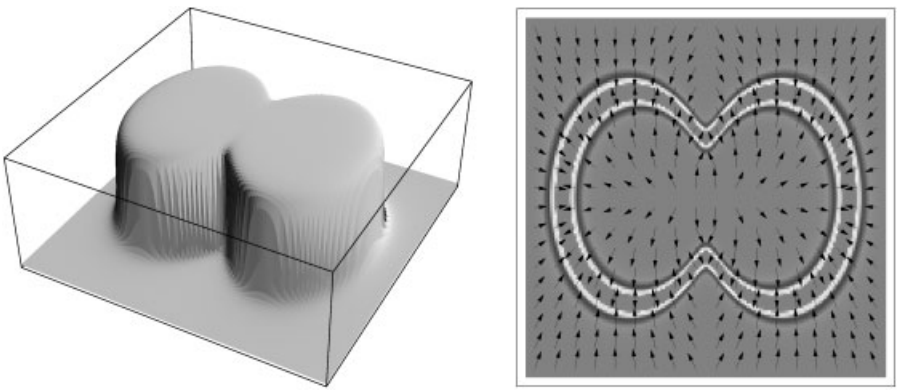

Figure 1. The image intensity function u_0 (left). The density plot of the function ϕ and corresponding vector field $\mathbf{W}$ (right).

equation on the interface. Following this approach and assuming a constant kinetic coefficient one obtains the equation

$$v = \gamma(v)k + F \tag{5}$$

describing the interface dynamics. It is often referred to as the *anisotropic curve shortening equation* with a constant driving force F (energy difference between bulk phases) and a given anisotropy function γ.

In the context of image segmentation, a problem is to detect plane curves on which the gradient ∇u_0 of the image intensity function $u_0 : R^2 \to [0,1]$ is large and which form boundaries of a segmented object. One can construct such a boundary by evolving a family of curves respecting the geometric equation (3) where $c = c(x,v)$ is a driving force and $\delta = \delta(x,v) > 0$ is a smoothing coefficient. We will use a generalization of a model proposed by Casseles *et al.* in Reference [3] and by Kichenassamy *et al.* in Reference [4]. To this end, let us take a smooth edge detector function $h : [0,\infty) \to (0,\infty)$ such that $h' < 0$, $h(0) = 1$, $h(+\infty) = 0$ and $h'(s) \leqslant Ch(s)$, $|h''(s)| \leqslant C$, $s > 0$, for some constant $C > 0$. A typical example of such a detector function is $h(s) = 1/(1 + \lambda s^2)$ where $\lambda > 0$ is a parameter (cf. Reference [25]). If the intensity function u_0 is C^2 smooth then the vector field $\mathbf{W}(x) = -\nabla\phi(x)$ where $\phi(x) = h(|\nabla u_0(x)|)$ has an important geometric property because it points towards regions where the norm of the gradient ∇u_0 is large (see Figure 1 right). Notice that a possible lack of smoothness of u_0 (e.g. due to a noise) can be overcome by convolving u_0 by a smooth mollifier G_σ having a compact support of a small radius $\sigma > 0$ or by applying a selectively smoothing non-linear filter [26,27]. Taking into account the geometric property of the vector field $\mathbf{W}(x)$ we are in a position to define a driving force $c(x,v)$ as follows:

$$c(x,v) = b(\phi(x))\mathbf{W}(x).\mathbf{N} = -b(\phi(x))\nabla\phi(x).\mathbf{N} \tag{6}$$

where $b = b(\phi)$ and the unit inward normal vector $\mathbf{N}$ is given by $\mathbf{N} = (-\sin v, \cos v)$. A reasonable choice of a regularization function δ, which will decrease the amount of regularization

in a neighbourhood of an edge, is given by

$$\delta(x) = a(\phi(x)) \tag{7}$$

where $a(\phi)$ is a smooth function, $a(0)=0$, $a(\phi)>0$ for $\phi>0$. As a typical example one can take $a(\phi)=\varepsilon\phi$ where $\varepsilon>0$ is a parameter. In the case $\varepsilon=1$ and $b(\phi)=1$ we obtain a model proposed and investigated in References [3,4].

3. ANALYSIS OF THE GOVERNING EQUATIONS

In this section, we derive a closed system of PDEs governing the evolution of the flow of plane curves satisfying the geometric equation (1). An embedded regular plane curve Γ will be parameterized by a smooth function $x: S^1 \to \mathbb{R}^2$ such that $\Gamma = \mathrm{Image}(x) = \{x(u), u \in [0,1]\}$ and $|\partial_u x| > 0$. Hereafter, we identify the unit circle S^1 with the interval $[0,1] \approx \mathbb{R}/\mathbb{Z}$ respecting the periodic boundary conditions at $u = 0, 1$. Let s denote the unit arc-length parameterization of a curve $\Gamma = \mathrm{Image}(x)$. Then $\mathrm{d}s = |\partial_u x|\mathrm{d}u$ and the tangent vector $\mathbf{T}$ and the signed curvature k of Γ satisfy

$$\mathbf{T} = \partial_s x = |\partial_u x|^{-1}\partial_u x, \quad k = \partial_s x \wedge \partial_s^2 x = |\partial_u x|^{-3}\partial_u x \wedge \partial_u^2 x \tag{8}$$

The unit inward normal vector $\mathbf{N}$ is chosen in such a way that $\mathbf{T} \wedge \mathbf{N} = 1$ where $\mathbf{a} \wedge \mathbf{b}$ is the determinant of the 2×2 matrix with column vectors $\mathbf{a}$, $\mathbf{b}$. By v we denote the tangent angle to Γ, i.e. $v = \arg(\mathbf{T})$. Then $(\cos v, \sin v) = \mathbf{T}$. By Frenét's formulae $\partial_s \mathbf{T} = k\mathbf{N}$ and $\partial_s \mathbf{N} = -k\mathbf{T}$.

Let a regular smooth initial curve $\Gamma_0 = \mathrm{Image}(x_0)$ be given. As it was already sketched in Section 1, a flow of plane curves $\Gamma_t = \mathrm{Image}(x(.,t))$, $t \in [0,T)$, satisfying (1) can be represented by a solution $x = x(u,t)$ to the position vector equation (2). Unfortunately, this equation cannot be solved directly because it contains the curvature k depending on higher order derivatives of a solution x itself (see (8)). This is why we have to construct a closed system of governing equations for the curvature k, the tangent angle v, the local length element $g = |\partial_u x|$ and the position vector x. The equations to follow are straightforward modifications of well-known geometric equations derived for the case of zero tangential velocity α (see e.g. References [11,28,29]). In the case $\alpha \neq 0$ these equations have been derived by the authors in Reference [21]. Recall that the equation for the tangential angle is: $\partial_t v = \partial_s \beta + \alpha k$. Since $\partial_s v = k$ and $\partial_s \beta = \beta'_k \partial_s k + \beta'_v k + \nabla_x \beta . \mathbf{T}$ we end up with the following closed system of parabolic-ordinary differential equations:

$$\partial_t k = \partial_s^2 \beta + \alpha \partial_s k + k^2 \beta \tag{9}$$

$$\partial_t v = \beta'_k \partial_s^2 v + (\alpha + \beta'_v)\partial_s v + \nabla_x \beta . \mathbf{T} \tag{10}$$

$$\partial_t g = -gk\beta + \partial_u \alpha \tag{11}$$

$$\partial_t x = \beta \mathbf{N} + \alpha \mathbf{T} \tag{12}$$

where $(u,t) \in [0,1] \times (0,T)$, $\mathrm{d}s = g\,\mathrm{d}u$ and $\mathbf{T} = \partial_s x = (\cos v, \sin v)$, $\mathbf{N} = \mathbf{T}^{\perp} = (-\sin v, \cos v)$. The functional α may depend on the variables k, v, g, x. A solution (k, v, g, x) to (9)–(12) is subject to initial conditions

$$k(.,0) = k_0, \quad v(.,0) = v_0, \quad g(.,0) = g_0, \quad (x.,0) = x_0(.)$$

and periodic boundary conditions at $u=0,1$ except for the tangent angle v for which we require that the tangent vector $\mathbf{T}(u,t)=(\cos(v(u,t)),\sin(v(u,t)))$ is 1-periodic in the u variable. Notice that the initial conditions for k_0, v_0, g_0 and x_0 (the curvature, tangent angle, local length element and position vector of the initial curve Γ_0) must satisfy the following compatibility constraints:

$$g_0=|\partial_u x_0|>0,\quad k_0=g_0^{-3}\partial_u x_0\wedge\partial_u^2 x_0,\quad \partial_u v_0=g_0k_0$$

In the rest of this section we will prove local in time existence of a classical solution of the governing system of Equations (9)–(12) by following the abstract theory of non-linear analytic semiflows due to Angenent (cf. Reference [30]). If we denote $\Phi=(k,v,g,x)$ then the system of governing Equations (9)–(12) can be rewritten as a fully non-linear PDE of the form

$$\partial_t\Phi=f(\Phi),\quad \Phi(0)=\Phi_0 \tag{13}$$

where $f(\Phi)=F(\Phi,\alpha(\Phi))$ and $F(\Phi,\alpha)$ is the right-hand side of (9)–(12). Let $0<\varrho<1$ be fixed. By E_k we denote the following scale of Banach spaces:

$$E_k=c^{2k+\varrho}(S^1)\times c_*^{2k+\varrho}(S^1)\times c^{1+\varrho}(S^1)\times(c^{2+\varrho}(S^1))^2 \tag{14}$$

where $k=0,\frac{1}{2},1$, and $c^{2k+\varrho}(S^1)$ is the 'little' Hölder space, i.e. the closure of $C^\infty(S^1)$ in the topology of the Hölder space $C^{2k+\varrho}(S^1)$ (see Reference [28]). By $c_*^{2k+\varrho}(S^1)$ we have denoted the Banach manifold $c_*^{2k+\varrho}(S^1)=\{v:\mathbb{R}\to\mathbb{R},\mathbf{T}=(\cos v,\sin v)\in(c^{2k+\varrho}(S^1))^2\}$. In order to overcome difficulties with function space setting one can treat equation (10) for the tangent angle v rewritten in terms of the tangent vector $\mathbf{T}$, i.e.

$$\partial_t\mathbf{T}=\partial_t v\mathbf{N}=\beta_k'\partial_s^2\mathbf{T}+\beta_k'k^2\mathbf{T}+(\alpha+\beta_v')\partial_s\mathbf{T}+(\nabla_x\beta.\mathbf{T})\mathbf{N}$$

where $\mathbf{N}=\mathbf{T}^\perp$. Clearly, $\mathbf{T}(.,t)\in(c^{2k+\varrho}(S^1))^2$ iff $v(.,t)c_*^{2k+\varrho}(S^1)$. Now if we assume

$$\alpha\in C^1(\mathcal{O}_{\frac{1}{2}},c^{2+\varrho}(S^1)) \tag{15}$$

for any bounded open subset $\mathcal{O}_{1/2}\subset E_{1/2}$ such that $g>0$ for any $(k,v,g,x)\in\mathcal{O}_{1/2}$ and the function $\beta:\mathbb{R}^2\times\mathbb{R}\times\mathbb{R}\to\mathbb{R}$ is C^4 smooth and 2π-periodic in the v variable then the mapping f is C^1 smooth from the open subset $\mathcal{O}_1=\mathcal{O}_{1/2}\cap E_1\subset E_1$ into E_0.

If the Fréchet derivative $df(\bar\Phi)\in\mathcal{L}(E_1,E_0)$ belongs to the maximal regularity class $\mathcal{M}_1(E_0,E_1)$ for any $\bar\Phi\in\mathcal{O}_1$ where $\mathcal{O}_1$ is a neighbourhood of the initial condition Φ_0 then, by Reference [30, Theorem 2.7], the abstract equation (13) has a unique solution $\Phi\in Y^{(T)}=C([0,T],E_1)\cap C^1([0,T],E_0)$ on some small enough time interval $[0,T]$. Recall that the class $\mathcal{M}_1(E_0,E_1)\subset\mathcal{L}(E_1,E_0)$ consists of those generators of analytic semigroups $A:D(A)=E_1\subset E_0\to E_0$ for which the linear equation $\partial_t\Phi=A\Phi+h(t)$, $0<t\leqslant1$, $\Phi(0)=\Phi_0$, has a unique solution $\Phi\in Y^{(1)}$ for any $h\in C([0,1],E_0)$ and $\Phi_0\in E_1$. In other words, (E_0,E_1) is a maximal parabolic regularity pair.

Theorem 3.1

Assume $\Phi_0=(k_0,v_0,g_0,x_0)\in E_1$ where k_0 is the curvature, v_0 is the tangential vector and $g_0=|\partial_u x_0|>0$ is the local length element of an initial regular curve $\Gamma_0=\mathrm{Image}(x_0)$. If $\beta=\beta(x,k,v)$ is a C^4 smooth function which is 2π-periodic in the v variable and such that

$\min_{\Gamma_0} \beta'_k(x_0,k_0,v_0)>0$. Suppose α satisfies (15). Then there exists a unique classical solution $\Phi=(k,v,g,x)\in C([0,T],E_1)\cap C^1([0,T],E_0)$ of governing system of Equations (9)–(12) defined on some small time interval $[0,T]$, $T>0$. Moreover, if Φ is the maximal solution defined on $[0,T_{\max}]$ then either $T_{\max}=+\infty$ or $\liminf_{t\to T_{\max}^-}\min_{\Gamma_t}\beta'_k(x,k,v)=0$ or $T_{\max}<+\infty$ and $\max_{\Gamma_t}|k|\to\infty$ as $t\to T_{\max}$.

Proof
Since $\partial_s v=k$ and $\partial_s\beta=\beta'_k\partial_s k+\beta'_v k+\nabla_x\beta.\mathbf{T}$ the curvature equation (9) can be rewritten in the divergent form

$$\partial_t k=\partial_s(\beta'_k\partial_s k)+\partial_s(\beta'_v k)+k\nabla_x\beta.\mathbf{N}+\partial_s(\nabla_x\beta.\mathbf{T})+\alpha\partial_s k+k^2\beta$$

Let us take an open bounded subset $\mathcal{O}_{1/2}\subset E_{1/2}$ such that $\Phi_0\in\mathcal{O}_1=\mathcal{O}_{1/2}\cap E_1\subset E_1$, $g>0$, and $\beta'_k(x,k,v)>0$ for any $(k,v,g,x)\in\mathcal{O}_1$. The linearization of f at a point $\bar\Phi=(\bar k,\bar v,\bar g,\bar x)\in\mathcal{O}_1$ has the form $df(\bar\Phi)=d_\Phi F(\bar\Phi,\bar\alpha)+d_\alpha F(\bar\Phi,\bar\alpha)d_\Phi\alpha(\bar\Phi)$ where $\bar\alpha=\alpha(\bar\Phi)$ and

$$d_\Phi F(\bar\Phi,\bar\alpha)=\partial_u\bar D\partial_u+\bar B\partial_u+\bar C,\quad d_\alpha F(\bar\Phi,\bar\alpha)=(\bar g^{-1}\partial_u\bar k,\bar k,\partial_u,\bar{\mathbf{T}})$$

$\bar D=\operatorname{diag}(\bar D_{11},\bar D_{22},0,0,0)$, $\bar D_{11}=\bar D_{22}=\bar g^{-2}\beta'_k(\bar x,\bar k,\bar v)\in C^{1+\varrho}(S^1)$ and $\bar B$, $\bar C$ are 5×5 matrices with $C^\varrho(S^1)$ smooth coefficients. Moreover, $\bar B_{ij}=0$ for $i=3,4,5$ and $\bar C_{3j}\in C^{1+\varrho}$, $\bar C_{ij}\in C^{2+\varrho}$ for $i=4,5$ and all j. The linear operator A_1 defined by $A_1\Phi=\partial_u(\bar D\partial_u\Phi)$, $D(A_1)=E_1\subset E_0$ is a generator of an analytic semigroup on E_0 and, moreover, $A_1\in\mathcal{M}_1(E_0,E_1)$ (see Reference [30]). Notice that $d_\alpha F(\bar\Phi,\bar\alpha)$ belongs to $\mathcal{L}(C^{2+\varrho}(S^1),E_{1/2})$ and this is why we can write $d_\Phi f(\bar\Phi)$ as a sum A_1+A_2 where $A_2\in L(E_{1/2},E_0)$. Thus $\|A_2\Phi\|_{E_0}\leqslant C\|\Phi\|_{E_{1/2}}\leqslant C\|\Phi\|_{E_0}^{1/2}\|\Phi\|_{E_1}^{1/2}$ and so the linear operator A_2 is a relatively bounded linear perturbation of A_1 with zero relative bound (cf. Reference [30]). With regard to Reference [30, Lemma 2.5] the class $\mathcal{M}_1$ is closed with respect to such perturbations. Thus $d_\Phi f(\bar\Phi)\in\mathcal{M}_1(E_0,E_1)$. The proof of the short time existence of a solution Φ now follows from [30, Theorem 2.7].

Finally, we will show that the maximal curvature becomes unbounded as $t\to T_{\max}$ in the case $\liminf_{t\to T_{\max}^-}\min_{\Gamma_t}\beta'_k>0$ and $T_{\max}<+\infty$. Suppose to the contrary that $\max_{\Gamma_t}|k|\leqslant M<\infty$ for any $t\in[0,T_{\max})$. According to [Reference [28], Theorem 3.1] there exists a unique maximal solution $\Gamma:[0,T'_{\max})\to\Omega(\mathbb{R}^2)$ satisfying the geometric equation (1). Recall that $\Omega(\mathbb{R}^2)$ is the space of C^1 regular Jordan curves in the plane (cf. Reference [28]). Moreover, Γ_t is a C^∞ smooth curve for any $t\in(0,T'_{\max})$ and the maximum of the absolute value of the curvature tends to infinity as $t\to T'_{\max}$. Thus $T_{\max}<T'_{\max}$ and therefore the curvature and subsequently v remain bounded in $C^{2+\varrho'}$ norm on the interval $[0,T_{\max}]$ for any $\varrho'\in(\varrho,1)$. Applying the compactness argument one sees that the limit $\lim_{t\to T_{\max}}\Phi(.,t)$ exists and remains bounded in the space E_1 and one can continue the solution Φ beyond $T_{\max}$, a contradiction. □

Remark 3.2
In a general case where the normal velocity may depend on the position vector x, the maximal time of existence of a solution can be either finite or infinite. Indeed, as an example one can consider the unit ball $B=\{|x|<1\}$ and function $\delta(x)=(|x|-1)^\gamma$ for $x\notin B$, $\gamma>0$. Suppose that $\Gamma_0=\{|x|=R_0\}$ is a circle with a radius $R_0>1$ and the family Γ_t, $t\in[0,T)$ evolves according to the normal velocity function $\beta(x,k)=\delta(x)k$. Then, it is an easy calculus to verify that the family Γ_t approaches the boundary $\partial B=\{|x|=1\}$ in a finite time $T_{\max}<\infty$ provided that $0<\gamma<1$ whereas $T_{\max}=+\infty$ in the case $\gamma=1$.

4. LYAPUNOV FUNCTIONALS AND QUALITATIVE PROPERTIES OF SOLUTIONS

In this section, we will analyse the qualitative properties of a solution to the governing system of Equations (9)–(12). The aim is to derive suitable Lyapunov functionals decreasing along trajectories as well as to prove *á priori* estimates of solutions to (9)–(12) for particular choices of the normal velocity functional α.

We begin with a well-known identity for the total length of evolving curves satisfying (1). Since α is periodic in the u variable we obtain from (11)

$$\frac{\mathrm{d}}{\mathrm{d}t} L_t + \int_{\Gamma_t} k\beta \,\mathrm{d}s = 0$$

where

$$L_t = \int_{\Gamma_t} \mathrm{d}s = \int_0^1 g(u,t)\,\mathrm{d}u \tag{16}$$

is the total length of a curve Γ_t. If $k\beta \geqslant 0$ then the evolution of plane curves parameterized by a solution of (2) represents a curve shortening flow, i.e. $L_{t_2} \leqslant L_{t_1} \leqslant L_0$ for any $0 \leqslant t_1 \leqslant t_2 \leqslant T$.

In the rest of this section we will only focus on the normal velocity function β arising from the image segmentation problem discussed in more detail in Section 2.2. We will assume that the normal velocity function $v = \beta(x,k,v)$ has the following form:

$$\beta(x,k,v) = a(\phi)k - b(\phi)(\nabla\phi.\mathbf{N}) \tag{17}$$

where $\phi = \phi(x)$ is a smooth and bounded (up to the second derivative) function, $\phi : \Omega \to (0,1]$ defined in a domain $\Omega \subset \mathbb{R}^2$ and $a = a(\phi), b = b(\phi)$ are smooth functions $a(\phi) > 0$ for $\phi > 0$.

Let us consider a flow Γ_t, $t \geqslant 0$, of plane curves with the normal velocity given by (17). Local in time existence of a smooth solution follows from Theorem 3.1 provided that the initial curve $\Gamma_0 \subset \Omega$ is smooth. Notice that

$$\phi(x) > 0 \quad \text{for any } x \in \Gamma_0 \tag{18}$$

In the following proposition we will show that the flow Γ_t, $t > 0$, has a gradient structure, i.e. there exists a Lyapunov functional non-increasing with respect to time t.

Proposition 4.1
If a family Γ_t, $0 \leqslant t < T_{\max}$, of plane curves satisfies (17) then

$$\frac{\mathrm{d}}{\mathrm{d}t} \int_{\Gamma_t} H(\phi(x))\,\mathrm{d}s + \int_{\Gamma_t} \frac{H(\phi(x))}{a(\phi(x))}\,\beta^2\,\mathrm{d}s = 0$$

where

$$H(\phi) = \mathrm{e}^{\int_0^\phi (b(\xi)/a(\xi))\,\mathrm{d}\xi} \tag{19}$$

In particular, the functional $V(\Gamma) = \int_\Gamma H(\phi(x))\,\mathrm{d}s$ is a Lyapunov functional, i.e. $(\mathrm{d}/\mathrm{d}t)V(\Gamma_t) \leqslant 0$ for any $0 \leqslant t < T_{\max}$.

Proof
Computing the time derivative of $H(\phi)$ we obtain: $\partial_t H(\phi) = H'(\phi)(\nabla\phi.\partial_t x) = (bH(\phi)/a)(\beta(\nabla\phi.\mathbf{N}) + \alpha(\nabla\phi.\mathbf{T})) = (bH(\phi)/a)\beta(\nabla\phi.\mathbf{N}) + \alpha\partial_s H(\phi)$ where $\phi = \phi(x)$, $a = a(\phi)$, $b = b(\phi)$, and $x = x(u,t)$ is a solution to (9)–(12) representing the curve Γ_t, i.e. $\Gamma_t = \text{Image}(x(.,t))$. Since $\mathrm{d}s = g\,\mathrm{d}u$ and $\partial_t g = -gk\beta + \partial_u\alpha$ we have

$$\frac{\mathrm{d}}{\mathrm{d}t}\int_{\Gamma_t} H(\phi)\,\mathrm{d}s = \int_{\Gamma_t} \partial_t H(\phi) - H(\phi)k\beta + H(\phi)\partial_s\alpha\,\mathrm{d}s$$
$$= \int_{\Gamma_t} \beta H(\phi)\left(\frac{b}{a}(\nabla\phi.\mathbf{N}) - k\right)\mathrm{d}s = -\int_{\Gamma_t}\frac{\beta^2}{a}H(\phi)\,\mathrm{d}s$$

because $\beta = ak - b(\nabla\phi.\mathbf{N})$ and $\int_{\Gamma_t}\alpha\partial_s H + H\partial_s\alpha\,\mathrm{d}s = \int_{\Gamma_t}\partial_s(\alpha H)\,\mathrm{d}s = 0$. □

As an immediate consequence of the previous result we can exclude the existence of time periodic families of plane curves with the normal velocity satisfying (17).

Corollary 4.1
There exists no non-trivial time periodic family of plane curves Γ_t, $t \geqslant 0$, satisfying (17).

The next result is focused on *á priori* estimates of solutions. We will need the following structural assumptions made on the functions a and ϕ:

$$\begin{aligned} &a(0) = 0, 0 < a(\phi) \leqslant C_1\phi \quad \text{for any } 0 < \phi \leqslant 1 \\ &|\nabla\phi(x)| \leqslant C_2\phi(x) \qquad\quad \text{for any } x \in \Omega \end{aligned} \tag{20}$$

where $C_1, C_2 > 0$ are positive constants. Notice that this hypothesis is fulfilled in the case $a(\phi) = \varepsilon\phi, \varepsilon > 0$ and the function ϕ is defined as in Section 2, i.e. $\phi(x) = h(|\nabla u_0(x)|)$ where $h : [0,\infty) \to [0,1]$ is an arbitrary edge detector function and u_0 is a smoothed image intensity function.

Lemma 4.2
Assume (20). If a family Γ_t, $0 \leqslant t < T_{\max}$, of plane curves satisfies (17) then there exists a constant $C > 0$ such that $\min_{x\in\Gamma_t}\phi(x) \geqslant \mathrm{e}^{-Ct}\min_{x\in\Gamma_0}\phi(x)$ for any $0 \leqslant t < T_{\max}$.

Proof
Let $z(u,t) = \phi(x(u,t))$ where $\Gamma_t = \text{Image}(x(.,t))$ and x is a solution to (9)–(12). With regard to (2) and Frenét's formulae it is an easy calculation to verify that z is a solution to the following parabolic equation:

$$\partial_t z = a(z)\partial_s^2 z - a(z)\mathbf{T}^T\nabla^2\phi\mathbf{T} + \alpha\partial_s z - b(z)(\nabla\phi.\mathbf{N})^2$$

where $a(z) = a(z(u,t)) \geqslant 0$, $b(z) = b(z(u,t))$. Since ϕ is assumed to be smooth it follows from (20) that there exist constants $C_3, C_4 > 0$ such that $|a(\phi(x))\mathbf{T}^T\nabla^2\phi(x)\mathbf{T}| \leqslant C_3\phi(x) = C_3 z$ and $|b(\phi(x))\|\nabla\phi(x)|^2 \leqslant C_4\phi(x) = C_4 z$. Since $|\nabla\phi(x)|^2 = (\nabla\phi(x).\mathbf{N})^2 + (\nabla\phi(x).\mathbf{T})^2 = (\nabla\phi(x).\mathbf{N})^2 + (\partial_s z)^2$ we have

$$\partial_t z \geqslant a\partial_s^2 z + (b(z)\partial_s z + \alpha)\partial_s z - Cz$$

for some constant $C>0$ depending on C_3 and C_4 only. Applying the parabolic maximum principle yields $\min_{u\in[0,1]} z(u,t)\geqslant \mathrm{e}^{-Ct}\min_{u\in[0,1]} z(u,0)$ for any $0\leqslant t<T_{\max}$ and the proof of lemma follows. □

As a consequence of the previous result we obtain

Proposition 4.3
Assume hypothesis (20) is fulfilled. If the normal velocity of an evolving family Γ_t, $0\leqslant t<T_{\max}$, of plane curves satisfies (17) then for the maximal time of existence of a solution we have either $T_{\max}=\infty$ or $T_{\max}<\infty$. If $T_{\max}<\infty$ then the modulus of the curvature $|k(.,t)|$ becomes unbounded and $L_t\to 0$ as $t\to T_{\max}$.

Proof
The proof follows from Theorem 3.1 and the previous lemma. □

5. CONTROLLING THE TANGENTIAL MOTION

The purpose of this section is to discuss the role of a tangential velocity functional α in equation (2) for the position vector. In comparison to the approach developed [21], where an initial distribution of grid points is preserved during evolution, the aim of this section is to generalize this approach in order to achieve uniform redistribution of points belonging to Γ_t.

The idea behind the construction of a suitable functional α is to examine the behaviour of the so-called relative local length defined as the ratio $g(u,t)/L_t$. If this ratio tends to some constant $C>0$ as $t\to T_{\max}$, i.e. $\lim_{t\to T_{\max}^-} g(u,t)/L_t=C$ then, at the maximal time $t=T_{\max}$ the redistribution of grid points becomes constant. Inevitably, the identity $\int_0^1 g(u,t)\,\mathrm{d}u = L_t$ implies $C=1$. Moreover, the condition

$$\lim_{t\to T_{\max}^-}\frac{g(u,t)}{L_t}=1$$

is fulfilled provided that there exists a relaxation function $\omega\in L^1_{\mathrm{loc}}[0,T_{\max}))$ such that

$$\int_0^{T_{\max}}\omega(\tau)\,\mathrm{d}\tau=\infty \tag{21}$$

and $g(u,t)/L_t=1+(g_0(u)/L_0-1)\mathrm{e}^{-\int_0^t\omega(\tau)\,\mathrm{d}\tau}$ for any $u\in[0,1]$ and $t\in[0,T_{\max})$. This equation can be rewritten as an ODE

$$\frac{\mathrm{d}}{\mathrm{d}t}\left(\frac{g(u,t)}{L_t}-1\right)+\omega(t)\left(\frac{g(u,t)}{L_t}-1\right)=0$$

Taking into account the local length equation (11) and total length equation (16) the above ODE is satisfied if and only if the tangential velocity functional α obeys the equation

$$\partial_u\alpha=g\left(k\beta-\frac{1}{L}\int_\Gamma k\beta\right)+\omega(t)(L-g) \tag{22}$$

where $L=L_t$ is the total length of the curve $\Gamma=\Gamma_t$.

5.1. Finite time extinction solutions

By a finite time extinction solution of the mean curvature flow we mean an evolving family of plane curves Γ_t existing on a maximal finite time interval $[0, T_{\max})$ where $T_{\max} < \infty$ and such that the total length L_t vanishes as $t \to T_{\max}^-$, i.e. $\lim_{t \to T_{\max}^-} L_t = 0$. It is always the case if the normal velocity β satisfies $\beta'_k(x,k,v) \geqslant \lambda,\ \beta(x,0,v) = 0$ for any x, k, v where $\lambda > 0$ is a constant. As an example one can consider the normal velocity of the form $\beta(x,k,v) = \delta(x,v)k$ where $\delta(x,v) \geqslant \lambda > 0$.

Let us define a relaxation function ω as follows:

$$\omega(t) = \frac{\kappa}{L_t} \int_{\Gamma_t} k\beta \, \mathrm{d}s \tag{23}$$

where $\kappa > 0$ is a positive constant. According to (16) we have

$$\int_0^t \omega(\tau) \, \mathrm{d}\tau = -\kappa \int_0^t \partial_\tau \ln L_\tau \, \mathrm{d}\tau = \kappa(\ln L_0 - \ln L_t) \to \infty \quad \text{as } t \to T_{\max}^-$$

Hence the relaxation function ω defined by (23) satisfies the structural condition (21). In this case Equation (22) has the form

$$\partial_u \alpha = g\left(k\beta - \frac{1+\kappa}{L} \int_\Gamma k\beta\right) + \kappa \int_\Gamma k\beta \tag{24}$$

Remark 5.1

If we formally set $\kappa = 0$ in (24) then we obtain the same equation for the tangential velocity α as the one derived in References [16,19,21, Equation (27)]. Recall that in this case the relative local length $g(u,t)/L_t$ is preserved, i.e. $g(u,t)/L_t = g_0(u)/L_0$ for any $u \in [0,1]$ and $t \in [0,T)$. On the other hand, taking $\kappa > 0$ yields $\lim_{t \to T_{\max}^-} g(u,t)/L_t = 1$ for any $u \in [0,1]$ independent of the initial redistribution of the local length $g_0 = |\partial_u x_0|$ at $t = 0$.

5.2. Image segmentation problem

In this section, we will study the case where the normal velocity function β arises from the image segmentation problem discussed in a more detail in Sections 2 and 4. We will suppose that the normal velocity function $v = \beta(x,k,v)$ has the form (17) with coefficients a, b and the structural hypothesis (20) is satisfied.

Let $\Gamma_t,\ 0 \leqslant t < T_{\max}$, be a solution to (1) existing on a maximal time interval $[0, T_{\max})$. With regard to Proposition 4.3 either $T_{\max} = \infty$ or $T_{\max} < \infty$. In the case $T_{\max} < \infty$ we furthermore have $L_t \to 0$ as $t \to T_{\max}^-$ and the function $\omega(t)$ defined as in (23) is a relaxation function. In the general case $T_{\max} \leqslant \infty$ let us define a function

$$\omega(t) = \kappa_1 + \frac{\kappa_2}{L_t} \int_{\Gamma_t} k\beta \, \mathrm{d}s \tag{25}$$

where $\kappa_1, \kappa_2 > 0$ are some positive constants. In order to clarify how κ_1 must be chosen with respect to κ_2 let us denote $B(\phi)$ a primitive function to $b(\phi)$, i.e. $B'(\phi) = b(\phi)$. From Frenet's

formula $\partial_s \mathbf{T} = k\mathbf{N}$ we have

$$-\int_{\Gamma_t} b(\phi(x))(\nabla\phi(x).\mathbf{N})k\,\mathrm{d}s = -\int_{\Gamma_t} (\nabla B(\phi(x)).\partial_s \mathbf{T})\,\mathrm{d}s$$
$$= \int_{\Gamma_t} \mathbf{T}^T \nabla^2 B(\phi(x))\mathbf{T}\,\mathrm{d}s \geqslant -C\int_{\Gamma_t} \mathrm{d}s = -C\,L_t$$

where $C>0$ is a constant such that $\max_{x\in\Omega} |\nabla^2 B(\phi(x))| \leqslant C$. Since

$$\int_{\Gamma_t} k\beta\,\mathrm{d}s = \int_{\Gamma_t} a(\phi(x))k^2 - b(\phi(x))\ (\nabla\phi(x).\mathbf{N})k\,\mathrm{d}s \geqslant -C\,L_t$$

we have $\int_0^{T_{\max}} \omega(t)\,\mathrm{d}t = \infty$ provided that $\kappa_1 > C\kappa_2$ irrespective of the fact as to whether $T_{\max} < \infty$ or $T_{\max} = \infty$. Hence ω can be used as a relaxation function.

Proposition 5.1
Up to an additive constant there exists a unique tangential velocity functional α satisfying (22) where the relaxation function ω is given by (25) with $\kappa_1, \kappa_2 \geqslant 0$. Moreover, $\alpha \in C^1(\mathcal{O}_{1/2}, c^{2+\varrho}(S^1))$ i.e. the tangential velocity functional α satisfies the condition (15).

Proof
The proof directly follows from the definition of the tangential velocity functional α (22) and basic properties of Hölder spaces. □

6. NUMERICAL SCHEMES AND RESULTS

First we consider the normal velocity

$$\beta = \beta(k, v) = \gamma(v)k + F \tag{26}$$

with a given anisotropy function $\gamma(v) > 0$ and a constant driving force F [13]. The system of governing equations is accompanied by the tangential velocity α given by Equation (22) with relaxation function ω discussed in Section 5.2. Since there is no explicit dependence of flow on spatial position x the governing equations are a bit simplified and the evolving curve Γ_t is given (uniquely up to a translation) by reconstruction

$$x(u,.) = \int_0^u g\mathbf{T}\,\mathrm{d}u = \int_0^s \mathbf{T}\,\mathrm{d}s \tag{27}$$

Before performing temporal and spatial discretization we insert (22) into (9) and (11) to obtain

$$\partial_t k = \partial_s^2 \beta + \partial_s(\alpha k) + k\,\frac{1}{L}\int_\Gamma k\beta\,\mathrm{d}s + k\omega\left(1 - \frac{L}{g}\right) \tag{28}$$

$$\partial_t v = \beta'_k \partial_s^2 v + (\alpha + \beta'_v)\partial_s v \tag{29}$$

$$\partial_t g = -g\,\frac{1}{L}\int_\Gamma k\beta\,\mathrm{d}s - \omega(g - L) \tag{30}$$

From the numerical discretization point of view, critical terms in Equations (9)–(11) are represented by the reaction term $k^2\beta$ in (9) and the decay term $k\beta$ in (11). In Equations (28)–(30) these critical terms were replaced by the averaged value of $k\beta$ along the curve, thus computation of a local element length in the neighbourhood of point with a high curvature is more stable.

In our computational method a solution of the evolution Equation (1) is represented by discrete plane points $x_i^j, i=0,\ldots,n,\ j=0,\ldots,m$, where index i represents space discretization and index j a discrete time stepping. Since we only consider closed initial curves the periodicity condition $x_0^0 = x_n^0$ is required at the beginning. If we take a uniform time step $\tau = T/m$ and a uniform division of the fixed parametrization interval $[0,1]$ with a step $h = 1/n$, a point x_i^j corresponds to $x(ih, j\tau)$. Difference equations will be given for discrete quantities $k_i^j, v_i^j, r_i^j, i=1,\ldots,n,\ j=1,\ldots,m$ representing piecewise constant approximations of the curvature, tangent angle and element length for the segment $[x_{i-1}^j, x_i^j]$, which we call *flowing control volume*, and for α_i^j representing tangential velocity of the flowing node x_i^{j-1}. We will also use dual volumes $[\tilde{x}_{i-1}^j, \tilde{x}_i^j],\ i=1,\ldots,n,\ j=1,\ldots,m$, where $\tilde{x}_i^j = (x_{i-1}^j + x_i^j)/2$. Then, at the jth discrete time level, $j=1,\ldots,m$, the approximation of a curve is given by

$$x_i^j = x_0^j + \sum_{l=1}^{i} r_l^j(\cos(v_l^j), \sin(v_l^j)), \quad i=1,\ldots,n \tag{31}$$

In order to construct a discretization scheme for solving (28)–(30) we consider time-dependent functions $k_i, v_i, r_i, x_i, \alpha_i$. Functions $k_i^j, v_i^j, r_i^j, x_i^j, \alpha_i^j$ described above, representing their values at time levels $t = j\tau$.

First we integrate Equation (22) at any time t over $[x_{i-1}, x_i]$. Using the Newton–Leibniz formula and constant approximation of the quantities inside flowing control volumes we obtain

$$\alpha_i - \alpha_{i-1} = r_i k_i \beta(k_i, v_i) - r_i B - \omega\left(r_i - \frac{L}{n}\right)$$

where $B = 1/L \int_\Gamma k\beta \, \mathrm{d}s$. By taking discrete time stepping, for *values of the tangential velocity* α_i^j we obtain

$$\begin{aligned} \alpha_i^j &= \alpha_{i-1}^j + r_i^{j-1} k_i^{j-1} \beta(k_i^{j-1}, v_i^{j-1}) - r_i^{j-1} B^{j-1} - \omega(r_i^{j-1} - M^{j-1}) \\ i &= 1,\ldots,n, \text{ with } \alpha_0^j = 0 \ (x_0^j \text{ is moving only in the normal direction}) \text{ where} \end{aligned} \tag{32}$$

$$M^{j-1} = \frac{1}{n} L^{j-1}, \quad L^{j-1} = \sum_{l=1}^{n} r_l^{j-1}, \quad B^{j-1} = \frac{1}{L^{j-1}} \sum_{l=1}^{n} r_l^{j-1} k_l^{j-1} \beta(k_l^{j-1}, v_l^{j-1}) \tag{33}$$

and $\omega = \kappa_1 + \kappa_2 B^{j-1}$, with input redistribution parameters κ_1, κ_2. Integrating Equation (30) gives us

$$\frac{\mathrm{d}r_i}{\mathrm{d}t} + r_i B + r_i \omega = \omega \frac{L}{n}$$

By taking backward time difference we obtain *update for local lengths*

$$r_i^j = \frac{r_i^{j-1} + \tau\omega M^{j-1}}{1 + \tau(B^{j-1} + \omega)}, \quad i=1,\ldots,n,\ r_0^j = r_n^j,\ r_{n+1}^j = r_1^j \tag{34}$$

We will use also local lengths of dual volumes, $q_i^j = (r_i^j + r_{i+1}^j)/2,\ i = 1, \ldots, n$. Subsequently, new local lengths are used for approximation of intrinsic derivatives in (28) and (29). Integrating the curvature equation (28) over $[x_{i-1}, x_i]$ we have

$$r_i \frac{\mathrm{d}k_i}{\mathrm{d}t} = [\partial_s B(k,v)]_{x_{i-1}}^{x_i} + [\alpha k]_{x_{i-1}}^{x_i} + k_i \left(r_i(B+\omega) - \omega \frac{L}{n} \right)$$

By replacing the time derivative by time difference, approximating k in nodal points by the average value of neighbouring segments and using semi-implicit approach we obtain a *tridiagonal system* with periodic boundary conditions imposed *for new discrete values of curvature*

$$a_i^j k_{i-1}^j + b_i^j k_i^j + c_i^j k_{i+1}^j = d_i^j, \quad i = 1, \ldots, n,\ k_0^j = k_n^j,\ k_{n+1}^j = k_1^j \tag{35}$$

$$a_i^j = \frac{\alpha_{i-1}^j}{2} - \frac{\gamma(v_{i-1}^{j-1})}{q_{i-1}^j}, \quad c_i^j = -\frac{\alpha_i^j}{2} - \frac{\gamma(v_{i+1}^{j-1})}{q_i^j}, \quad d_i^j = \frac{r_i^j}{\tau} k_i^{j-1}$$

$$b_i^j = r_i^j \left(\frac{1}{\tau} - (B^{j-1} + \omega) \right) + \omega M^{j-1} - \frac{\alpha_i^j}{2} + \frac{\alpha_{i-1}^j}{2} + \frac{\gamma(v_i^{j-1})}{q_{i-1}^j} + \frac{\gamma(v_i^{j-1})}{q_i^j}$$

Finally, by integrating the tangent angle equation (29) we obtain

$$r_i \frac{\mathrm{d}v_i}{\mathrm{d}t} = \gamma(v_i)[\partial_s v]_{x_{i-1}}^{x_i} + [\alpha v]_{x_{i-1}}^{x_i} - v_i(\alpha_i - \alpha_{i-1}) + \gamma'(v_i) k_i [v]_{x_{i-1}}^{x_i}$$

By a similar approach as above we obtain a *tridiagonal system* with periodic boundary conditions *for new values of the tangent angle*

$$A_i^j v_{i-1}^j + B_i^j v_i^j + C_i^j v_{i+1}^j = D_i^j, \quad i = 1, \ldots, n, v_0^j = v_n^j - 2\pi, v_{n+1}^j = v_1^j + 2\pi \tag{36}$$

$$A_i^j = \frac{\alpha_{i-1}^j}{2} + \frac{\gamma'(v_i^{j-1}) k_i^j}{2} - \frac{\gamma(v_i^{j-1})}{q_{i-1}^j}, \quad B_i^j = \frac{r_i^j}{\tau} - (A_i^j + C_i^j)$$

$$C_i^j = -\frac{\alpha_i^j}{2} + \frac{\gamma'(v_i^{j-1}) k_i^j}{2} - \frac{\gamma(v_i^{j-1})}{q_i^j}, \quad D_i^j = \frac{r_i^j}{\tau} v_i^{j-1}$$

The initial quantities for the algorithm are computed as follows:

$$\begin{aligned}
R_i^0 &= (R_{i_1}^0, R_{i_2}^0) = x_i^0 - x_{i-1}^0, \quad i = 1, \ldots, n,\ R_0^0 = R_n^0,\ R_{n+1}^0 = R_1^0 \\
r_i^0 &= |R_i^0|, \quad i = 0, \ldots, n+1 \\
k_i^0 &= \frac{1}{2r_i^0} \operatorname{sgn}(R_{i-1}^0 \wedge R_{i+1}^0) \arccos\left(\frac{R_{i+1}^0 . R_{i-1}^0}{r_{i+1}^0 r_{i-1}^0} \right), \quad i = 1, \ldots, n \\
v_0^0 &= \arccos(R_{0_1}^0 / r_0^0) \text{ if } R_{0_2}^0 \geqslant 0, \quad v_0^0 = 2\pi - \arccos(R_{0_1}^0 / r_0^0) \text{ if } R_{0_2} < 0 \\
v_i^0 &= v_{i-1}^0 + r_i^0 k_i^0,\ i = 1, \ldots, n
\end{aligned} \tag{37}$$

Remark 6.1 (*Solvability and stability of the scheme*)
Let us first examine discrete values of the tangent angle computed from (36). One can rewrite it in the form

$$v_i^j + \frac{\tau}{r_i^j} C_i^j (v_{i+1}^j - v_i^j) + \frac{\tau}{r_i^j} A_i^j (v_{i-1}^j - v_i^j) = v_i^{j-1} \tag{38}$$

Let $\max_k v_k^j$ be attained at the ith node. We can always take a fine enough resolution of the curve, i.e. take small $q_i^j \ll 1$, $i = 1, \ldots, n$, such that both A_i^j and C_i^j are non-positive and thus the second and third terms on the left-hand side of (38) are non-negative. Then $\max_k v_k^j = v_i^j \leqslant v_i^{j-1} \leqslant \max_k v_k^{j-1}$. By a similar argument we can derive an inequality for minimum. In this way we have shown the L^∞-stability criterion, namely

$$\min_k v_k^0 \leqslant \min_k v_k^j \leqslant \max_k v_k^j \leqslant \max_k v_k^0, \quad j = 1, \ldots, m \tag{39}$$

Having guaranteed non-positivity of A_i^j and C_i^j we can conclude positivity and diagonal dominance of the diagonal term B_i^j. In particular, it implies that the tridiagonal matrix of the system (36) is an M-matrix and hence a solution to (36) always exists and is unique.

In the same way, by taking q_i^j small enough, we can prove the non-positivity of the off-diagonal terms a_i^j and c_i^j in system (35) for discrete curvature values. Then the diagonal term b_i^j is positive and dominant provided that $\tau(B^{j-1} + \omega) < 1$. Again we have shown that the corresponding matrix is an M-matrix and therefore there exists a unique solution to system (35).

Another natural stability requirement of the scheme is related to the positivity of local lengths r_i^j during computations. It follows from (34) that the positivity of r_i^j is equivalent to the condition $\tau(B^{j-1} + \omega) > -1$. Taking into account both inequalities for the time step we end up with the following stability restriction on the time step τ:

$$\tau \leqslant \frac{1}{|B^{j-1} + \omega|} \tag{40}$$

related to B^{j-1} (a discrete average value of $k\beta$ over a curve).

In the following figures we present numerical solutions computed by the scheme; initial curves are plotted with a thick line and the numerical solution is given by further solid lines with points representing the motion of some grid points during the curve evolution. In Figure 2 we compare computations with and without tangential redistribution for a large driving force F. As an initial curve we chose $x_1(u) = \cos(2\pi u)$, $x_2(u) = 2\sin(2\pi u) - 1.99\sin^3(2\pi u)$, $u \in [0, 1]$. Without redistribution, the computations are collapsing soon because of the degeneracy in local element lengths in parts of a curve with high curvature leading to a merging of the corresponding grid points. Using the redistribution the evolution can be successfully handled. We used $\tau = 0.00001$, 400 discrete grid points and we plotted every 150th time step. In Figure 3 we have considered an initial curve $x_1(u) = (1 - C\cos^2(2\pi u))\cos(2\pi u)$, $x_2(u) = (1 - C\cos^2(2\pi u))\sin(2\pi u)$, $u \in [0, 1]$ with $C = 0.7$. We took $\tau = 0.00001$ and 800 (Figure 3 left) and 1600 (Figure 3 right) grid points for representation of a curve. In Figure 3, left, we plot each 500th time step, and in Figure 3, right, each 100th step. It is natural that we have to use small time steps in the case of a strong driving force. However, the time step is not restricted by the point-wise values of the almost

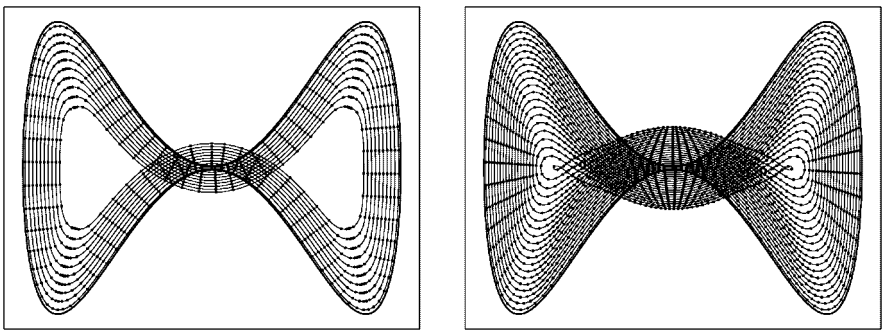

Figure 2. Isotropic curvature driven motion, $\beta(k,v)=\varepsilon k+F$, with $\varepsilon=1$, $F=10$, without (left) and with (right) uniform tangential redistribution of grid points.

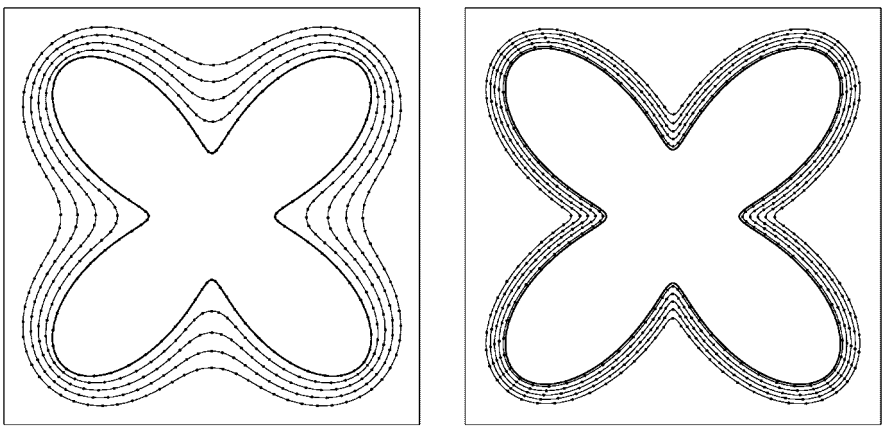

Figure 3. Isotropic curvature driven motion of an initial non-convex curve including uniform tangential redistribution of grid points; $\beta(k,v)=\varepsilon k+F$, with $\varepsilon=1$, $F=-10$ (left) and $\varepsilon=0.1$, $F=-10$ (right). Resolution of sharp corners in the case of a highly dominant forcing term using the algorithm with redistribution is possible.

singular curvature in the corners which would lead to an unrealistic time step restriction. According to (40), the time step is restricted by the average value of $k\beta$ computed over the curve which is much more weaker restriction because of the regularity of the curve outside the corners. In Figure 4 we present experiments with three-fold anisotropy starting with unit circle. We used $\tau=0.001$, 300 grid points and we plotted every 50th time step (left) and every 750th time step (right). In all experiments including redistribution, the parameters $\kappa_1=\kappa_2=10$.

Now we shall consider the motion of the curves with explicit dependence of the flow on position x and suggest a numerical scheme for such a situation. Since we consider (1) with a linear dependence of β on curvature (3) by using Frenet's formulae one can rewrite the position vector Equation (12) as an intrinsic convection–diffusion equation for the vector x

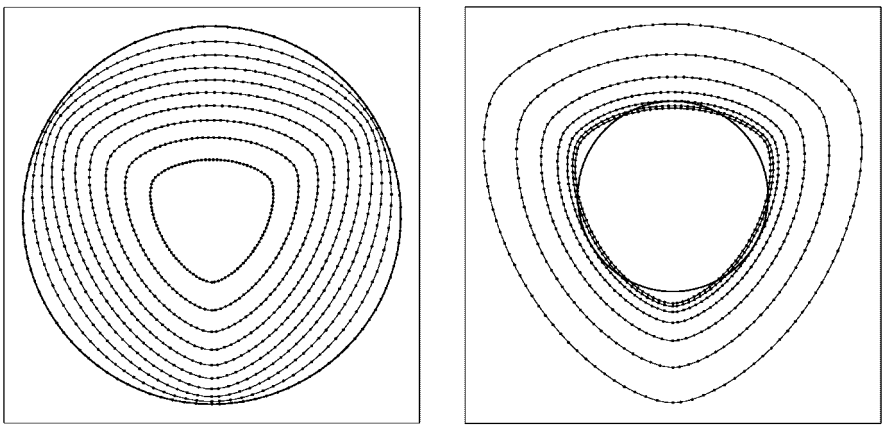

Figure 4. Anisotropic curvature driven motion of the initial unit circle including uniform tangential redistribution of grid points; $\beta(k,v)=\gamma(v)k+F$, with $\gamma(v)=1-\frac{7}{9}\cos(3v)$, $F=0$ (left) and $\gamma(v)=1-\frac{7}{9}\cos(3v)$, $F=-1$ (right).

and we obtain the system

$$\partial_t k=\partial_s^2\beta+\partial_s(\alpha k)+k\frac{1}{L}\int_\Gamma k\beta\,\mathrm{d}s+k\omega\left(1-\frac{L}{g}\right) \tag{41}$$

$$\partial_t v=\beta_k'\partial_s^2 v+(\alpha+\beta_v')\partial_s v+\nabla_x\beta.\mathbf{T} \tag{42}$$

$$\partial_t g=-g\frac{1}{L}\int_\Gamma k\beta\,\mathrm{d}s-\omega(g-L) \tag{43}$$

$$\partial_t x=\delta(x,v)\partial_s^2 x+\alpha\partial_s x+\mathbf{c}(x,v) \tag{44}$$

where $\beta=\beta(x,k,v)=\delta(x,v)k+c(x,v)$ and $\mathbf{c}(x,v)=(-c(x,v)\sin v,\ c(x,v)\cos v)$. In comparison to the scheme given above, two new tridiagonal systems have to be solved at each time level to update the curve position vector x. In order to construct a discretization scheme, Equations (41)–(43) together with (22) are integrated over $[x_{i-1},x_i]$ and the last Equation (44) over $[\tilde{x}_{i-1},\tilde{x}_i]$. Then, for *values of the tangential velocity* we obtain

$$\begin{aligned}\alpha_i^j=\alpha_{i-1}^j+r_i^{j-1}k_i^{j-1}\beta(\tilde{x}_i^{j-1},k_i^{j-1},v_i^{j-1})-r_i^{j-1}B^{j-1}\\ -\omega(r_i^{j-1}-M^{j-1}),\quad i=1,\ldots,n,\ \alpha_0^j=0\end{aligned} \tag{45}$$

with M^{j-1}, L^{j-1}, ω given as above and

$$B^{j-1}=\frac{1}{L^{j-1}}\sum_{l=1}^{n}r_l^{j-1}k_l^{j-1}\beta(\tilde{x}_l^{j-1},k_l^{j-1},v_l^{j-1}) \tag{46}$$

Local lengths are updated by the formula

$$r_i^j = \frac{r_i^{j-1} + \tau\omega M^{j-1}}{1 + \tau(B^{j-1} + \omega)}, \quad i = 1, \ldots, n, \;\; r_0^j = r_n^j, \;\; r_{n+1}^j = r_1^j \tag{47}$$

The *tridiagonal system for discrete values of the curvature* reads as follows:

$$a_i^j k_{i-1}^j + b_i^j k_i^j + c_i^j k_{i+1}^j = d_i^j, \quad i = 1, \ldots, n, \;\; k_0^j = k_n^j, \;\; k_{n+1}^j = k_1^j \tag{48}$$

$$a_i^j = \frac{\alpha_{i-1}^j}{2} - \frac{\delta(\tilde{x}_{i-1}^{j-1}, v_{i-1}^{j-1})}{q_{i-1}^j}, \quad c_i^j = -\frac{\alpha_i^j}{2} - \frac{\delta(\tilde{x}_{i+1}^{j-1}, v_{i+1}^{j-1})}{q_i^j}$$

$$b_i^j = r_i^j \left(\frac{1}{\tau} - (B^{j-1} + \omega) \right) + \omega M^{j-1} - \frac{\alpha_i^j}{2} + \frac{\alpha_{i-1}^j}{2} + \frac{\delta(\tilde{x}_i^{j-1}, v_i^{j-1})}{q_{i-1}^j} + \frac{\delta(\tilde{x}_i^{j-1}, v_i^{j-1})}{q_i^j}$$

$$d_i^j = \frac{r_i^j}{\tau} k_i^{j-1} + \frac{c(\tilde{x}_{i+1}^{j-1}, v_{i+1}^{j-1}) - c(\tilde{x}_i^{j-1}, v_i^{j-1})}{q_i^j} - \frac{c(\tilde{x}_i^{j-1}, v_i^{j-1}) - c(\tilde{x}_{i-1}^{j-1}, v_{i-1}^{j-1})}{q_{i-1}^j}$$

The *tridiagonal system for new values of the tangent angle* is given by

$$A_i^j v_{i-1}^j + B_i^j v_i^j + C_i^j v_{i+1}^j = D_i^j, \quad i = 1, \ldots, n, v_0^j = v_n^j - 2\pi, v_{n+1}^j = v_1^j + 2\pi \tag{49}$$

$$A_i^j = \frac{\alpha_{i-1}^j + \beta_v'(\tilde{x}_i^{j-1}, k_i^j, v_i^{j-1})}{2} - \frac{\delta(\tilde{x}_i^{j-1}, v_i^{j-1})}{q_{i-1}^j}$$

$$C_i^j = -\frac{\alpha_i^j + \beta_v'(\tilde{x}_i^{j-1}, k_i^j, v_i^{j-1})}{2} - \frac{\delta(\tilde{x}_i^{j-1}, v_i^{j-1})}{q_i^j}$$

$$B_i^j = \frac{r_i^j}{\tau} - (A_i^j + C_i^j), \quad D_i^j = \frac{r_i^j}{\tau} v_i^{j-1} + r_i^j \nabla_x \beta(\tilde{x}_i^{j-1}, v_i^{j-1}, k_i^j).(\cos(v_i^{j-1}), \sin(v_i^{j-1}))$$

Finally, we end up with *two tridiagonal systems for updating the position vector*

$$\mathscr{A}_i^j x_{i-1}^j + \mathscr{B}_i^j x_i^j + \mathscr{C}_i^j x_{i+1}^j = \mathscr{D}_i^j, \quad i = 1, \ldots, n, \;\; x_0^j = x_n^j, \;\; x_{n+1}^j = x_1^j \tag{50}$$

$$\mathscr{A}_i^j = -\frac{\delta(\tilde{x}_i^{j-1}, \frac{1}{2}(v_i^j + v_{i+1}^j))}{r_i^j} + \frac{\alpha_i^j}{2}, \quad \mathscr{C}_i^j = -\frac{\delta(\tilde{x}_i^{j-1}, \frac{1}{2}(v_i^j + v_{i+1}^j))}{r_{i+1}^j} - \frac{\alpha_i^j}{2}$$

$$\mathscr{B}_i^j = \frac{q_i^j}{\tau} - (\mathscr{A}_i^j + \mathscr{C}_i^j), \quad \mathscr{D}_i^j = \frac{q_i^j}{\tau} x_i^{j-1} + q_i^j \mathbf{c}\left(x_i^{j-1}, \frac{1}{2}(v_i^j + v_{i+1}^j) \right)$$

The *initial quantities* for the algorithm are given by (37).

In Figure 5 we consider $\delta(x, v) = (1 - 8/9 \cos(3v))(x_1^2 + x_2^2)$, $c(x, v) = x_1 \sin v - x_2 \cos v - 0.5$. We used 100 grid points representing a curve, time step $\tau = 0.001$ and redistribution parameters

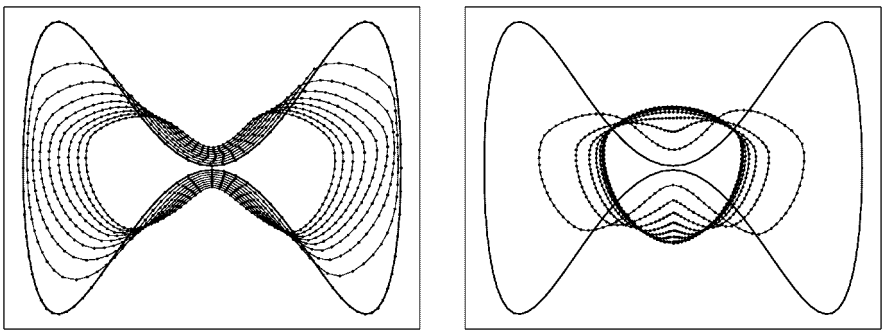

Figure 5. Curve evolution governed by $v=(1-8/9\ \cos(3v))(x_1^2+x_2^2)k+(-x_1,-x_2).(-\sin\ v,\cos\ v)-0.5$.

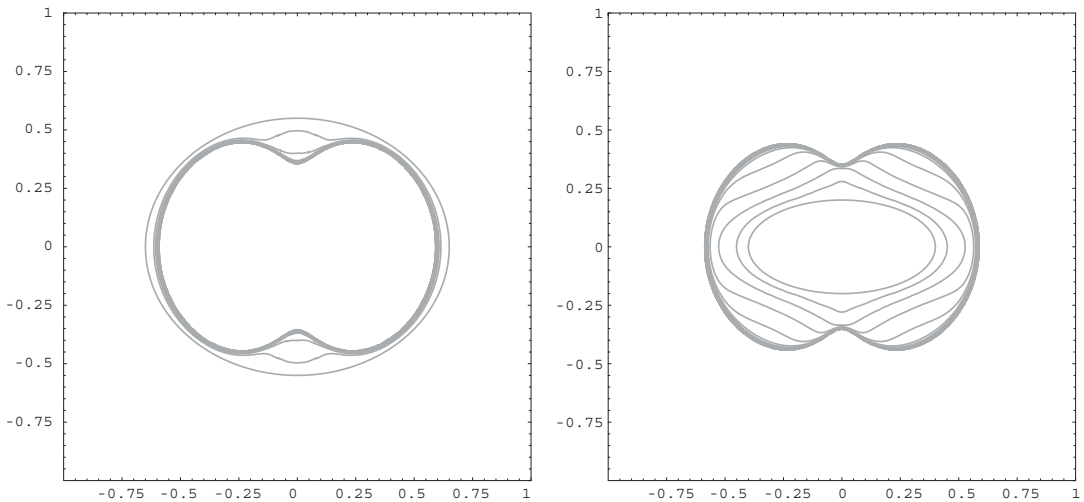

Figure 6. Convergence of an initial curve to the edge, from outside (left) and from inside (right).

$\kappa_1=\kappa_2=10$. In the left we plot an initial curve and then each 25th time step until the time $t=0.2$. In the right we continue visualization starting at time $t=0.2$ and then plotting each 200th time step until the time $t=1.6$, where we can see convergence to an anisotropic asymptotical shape.

Next we apply the computational method to the image segmentation problem, where $v=\varepsilon\ \phi(x)k-b(\phi(x))\nabla\phi(x).\mathbf{N}$, with $\phi(x)=h(|\nabla u_0(x)|),\ h(s)=1/(1+s^2)$. We consider an artificial image with the intensity function u_0 (see Figure 1 (left) and Figure 7 (right)) given by

$$u_0(x_1,x_2)=0.5+\frac{1}{10\pi}\,\mathrm{arctg}\left(12.5-\frac{100(x_1^2+x_2^2)}{(1+(x_1^2/(1.5x_1^2+0.5x_2^2)))^2}\right) \tag{51}$$

We have inserted an initial curve (an ellipse) with a resolution of 400 grid points inside the image, either to the exterior of a Jordan curve representing the edge (Figure 6 left), in its interior (Figure 6 right), or the initial ellipse crossing the edge (Figure 7 left). In all three

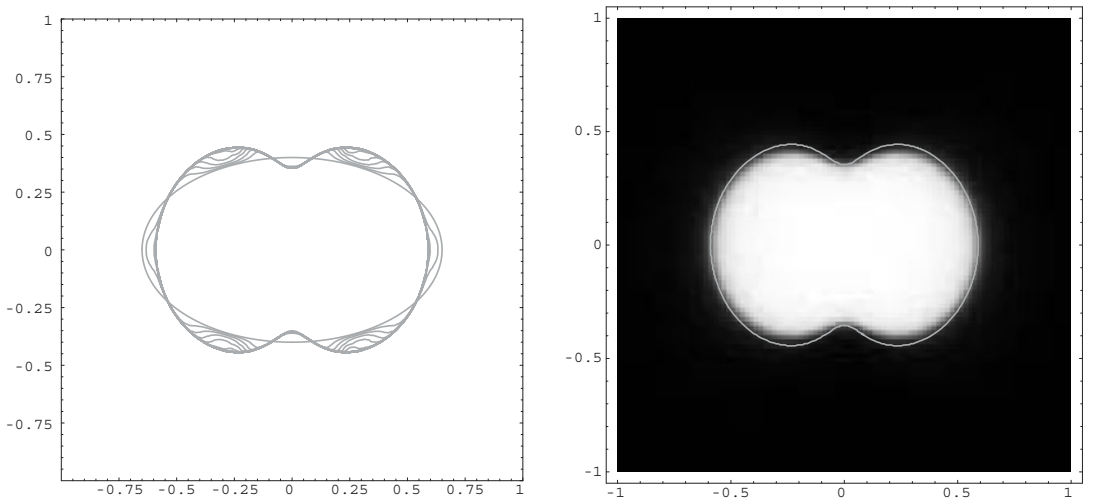

Figure 7. Convergence to the edge of an initial curve crossing the edge (left); the density plot of the image intensity function together with the limiting curve representing the edge position (right).

cases we can see convergence of the initial curve to the curve representing the edge position and all limiting curves coincide up to a very high level of accuracy. Naturally, the most fast segmentation was obtained in the third experiment. In the computations we have used the time step $\tau = 0.0001$, $\kappa_1 = \kappa_2 = 10$ and we evolved the initial curve until variations in the length and enclosed area are less than a prescribed tolerance (10^{-5}). We considered $\varepsilon = 0.1$ and $b(\phi(x)) = 0.5/1 - \phi(x) + \min_x \phi(x)$. A function b was suitably chosen in order to achieve a faster evolution of the curve in 'nearly flat' regions of the image.

ACKNOWLEDGEMENTS

This work was supported by grants VEGA No. 1/0313/03, No. 1/0259/03 and by SFB 359: Reactive Flows, Diffusion and Transport. The first author would like to thank Professor Willi Jäger for invitation to IWR, University of Heidelberg, where a substantial part of this work has been completed.

REFERENCES

1. Alvarez L, Guichard F, Lions PL, Morel JM. Axioms and fundamental equations of image processing. *Archives for Rational Mechanics and Analysis* 1993; **123**:200–257.
2. Sapiro G, Tannenbaum A. On affine plane curve evolution. *Journal of Functional Analysis* 1994; **119**:79–120.
3. Caselles V, Kimmel R, Sapiro G. Geodesic active contours. *International Journal of Computer Vision* 1997; **22**:61–79.
4. Kichenassamy S, Kumar A, Olver P, Tannenbaum A, Yezzi A. Conformal curvature flows: from phase transitions to active vision. *Archives for Rational Mechanics and Analysis* 1996; **134**:275–301.
5. Sethian JA. *Level Set Methods and Fast Marching Methods: Evolving Interfaces in Computational Geometry, Fluid Mechanics, Computer Vision, and Material Science*. Cambridge University Press: New York, 1999.
6. Sapiro G. *Geometric Partial Differential Equations and Image Analysis*. Cambridge University Press: Cambridge, 2001.
7. Osher S, Fedkiw R. *Level Set Methods and Dynamic Implicit Surfaces*. Springer: Berlin, 2003.
8. Osher S, Sethian J. Fronts propagating with curvature dependent speed: algorithm based on Hamilton-Jacobi formulation. *Journal of Computational Physics* 1988; **79**:12–49.

9. Nochetto R, Paolini M, Verdi C. Sharp error analysis for curvature dependent evolving fronts. *Mathematical Models and Methods in Applied Sciences* 1993; **3**:711–723.
10. Beneš M. Mathematical and computational aspects of solidification of pure crystallic materials. *Acta Mathematica Universitatis Comenianae* 2001; **70**:123–151.
11. Gage M, Hamilton RS. The heat equation shrinking convex plane curves. *Journal of Differential Geometry* 1986; **23**:69–96.
12. Grayson M. The heat equation shrinks embedded plane curves to round points. *Journal of Differential Geometry* 1987; **26**:285–314.
13. Angenent SB, Gurtin ME. Multiphase thermomechanics with an interfacial structure 2. Evolution of an isothermal interface. *Archives for Rational Mechanics and Analysis* 1989; **108**:323–391.
14. Dziuk G. Convergence of a semi discrete scheme for the curve shortening flow. *Mathematical Models and Methods in Applied Sciences* 1994; **4**:589–606.
15. Dziuk G. Discrete anisotropic curve shortening flow. *SIAM Journal on Numerical Analysis* 1999; **36**: 1808–1830.
16. Hou TY, Lowengrub J, Shelley M. Removing the stiffness from interfacial flows and surface tension. *Journal of Computational Physics* 1994; **114**:312–338.
17. Kimura M. Numerical analysis for moving boundary problems using the boundary tracking method. *Japan Journal of Industrial and Applied Mathematics* 1997; **14**:373–398.
18. Deckelnick K. Weak solutions of the curve shortening flow. *Calculus of Variations and Partial Differential Equations* 1997; **5**:489–510.
19. Hou TY, Klapper I, Si H. Removing the stiffness of curvature in computing 3-d filaments. *Journal of Computational Physics* 1998; **143**:628–664.
20. Mikula K, Ševčovič D. Solution of nonlinearly curvature driven evolution of plane curves. *Applied Numerical Mathematics* 1999; **31**:191–207.
21. Mikula K, Ševčovič D. Evolution of plane curves driven by a nonlinear function of curvature and anisotropy. *SIAM Journal on Applied Mathematics* 2001; **61**:1473–1501.
22. Mikula K, Kačur J. Evolution of convex plane curves describing anisotropic motions of phase interfaces. *SIAM Journal on Scientific Computing* 1996; **17**:1302–1327.
23. Mikula K. Solution of nonlinear curvature driven evolution of plane convex curves. *Applied Numerical Mathematics* 1997; **21**:1–14.
24. Schmidt A. Computation of three dimensional dendrites with finite elements. *Journal of Computational Physics* 1996; **125**:293–312.
25. Perona P, Malik J. Scale space and edge detection using anisotropic diffusion. *Proceedings of IEEE Computer Society Workshop on Computer Vision*, 1987.
26. Catté V, Lions PL, Morel JM, Coll T. Image selective smoothing and edge detection by nonlinear diffusion. *SIAM Journal on Numerical Analysis* 1992; **29**:182–193.
27. Kačur J, Mikula K. Solution of nonlinear diffusion appearing in image smoothing and edge detection. *Applied Numerical Mathematics* 1995; **17**:47–59.
28. Angenent SB. Parabolic equations for curves on surfaces I: curves with p-integrable curvature. *Annals of Mathematics* 1990; **132**:451–483.
29. Angenent SB. Parabolic equations for curves on surfaces II: intersections, blow-up and generalized solutions. *Annals of Mathematics* 1991; **133**:171–215.
30. Angenent SB. Nonlinear analytic semiflows. *Proceedings of Royal Society of Edinburgh, Section A* 1990; **115**:91–107.
31. Caselles V, Catté F, Coll T, Dibos F. A geometric model for active contours in image processing. *Numerische Matematik* 1993; **66**:1–31.
32. Malladi R, Sethian J, Vemuri B. Shape modeling with front propagation: a level set approach. *IEEE Transactions on Pattern Analysis and Machine Intelligence* 1995; **17**:158–174.

